Inorg. Chem. **1993,** *32,* 4337–4344

Ferromagnetism in the α and β Polymorphs of Anhydrous Copper(II) Formate: Two Molecular-Based Ferromagnets with Ordering Temperatures of 8.2 and 30.4 K

Fernando Sapiña,* Marcelino Burgos, Emilio Escrivá, José-Vicente Folgado, Dolores Marcos, Aurelio Beltrán, and Daniel Beltrán

UIBCM, Departament de Química Inorgànica, Facultat de Ciències Químiques, Universitat de València, c/ Dr. Moliner 50, 46100 Burjassot, València, Spain

Received March 17, 1993®

The first direct synthesis, the crystal structure, and the magnetic properties of one polymorph of anhydrous copper(II) formate, the β-[Cu(HCOO)$_2$] phase, as well as the magnetic characterization of the α-[Cu(HCOO)$_2$] phase, we reported in this work. β-[Cu(HCOO)$_2$] crystallizes in the monoclinic system, space group $P2_1/a$ (No. 14), with $Z = 2$ and cell parameters $a = 8.187(2)$ Å, $b = 7.922(2)$ Å, $c = 3.616(6)$ Å, $\beta = 122.14(2)°$ and $V = 194.6(5)$ Å^3. Least-squares refinement of 795 reflections ($I > 3\sigma(I)$) and 35 parameters gave a final $R = 0.044$. The structure comprises infinite bis(μ-oxo-ligand)-bridged chains of edge-sharing [CuO$_6$] elongated octahedra, running parallel to the [001] axis. Each chain is connected to four adjacent ones through carboxylate groups leading to a three dimensional network. The β phase is metastable and slowly transforms into the α one at room temperature. A mechanism for the $\beta \rightarrow \alpha$ transformation is proposed. Microwave absorption (MAMMA) experiments show that both α and β phases achieve 3d magnetic order near 10 and 30 K, respectively. These two polymorphs of anhydrous copper(II) formate present unusual magnetic properties, which have been characterized through ac and dc susceptibility as well as magnetization measurements. α-[Cu(HCOO)$_2$] shows ferromagnetic order at $T_c = 8.2$ K, and β-[Cu(HCOO)$_2$] behaves as a weak ferromagnet with $T_c = 30.4$ K. The magnetic behavior of both phases can be analyzed in terms of a 2d square planar Heisenberg model. The intralayer interaction results to be $J/k = 4.3$ K and $J/k = -41.4$ K and the interlayer one has been estimated (molecular field) to be $J_z/k = 0.38$ and $J_z/k = 0.64$ K for the α and β phases respectively.

Introduction

In the past few years there has been great interest in the study of the magnetic properties of molecular-based compounds, mainly when dealing with those exhibiting spontaneous magnetization below a critical temperature (molecular-based ferromagnets).[1]

Spontaneous magnetization only may result from one of the three following situations: (a) existence of ferromagnetic order between the individual magnetic moments; (b) existence of antiferromagnetic order but with a small canting, this resulting in a noncompensated moment in one direction of the crystal lattice (weak ferromagnetism); (c) long-range ferrimagnetic order. Whereas in this last case the presence of different magnetic sublattices is needed, this condition is not a requirement for situations a and b. However, insofar as the symmetry requisites for both case a (strict orthogonality between the magnetic orbitals in the crystal lattice) and case b (a relative arrangement of the magnetic atoms able to give antisymmetric exchange) are hardly fulfilled, the number of well-characterized examples of ferromagnetism and weak ferromagnetism known up to now is limited.[1,2]

Representative examples of these behaviors have been found in several families of compounds. If ordered bimetallic systems are considered, ferro and ferrimagnetic ordering has been observed in cyanide-based compounds,[3] whereas ferrimagnetic ordering is shown by complexes involving organic ligands[4,5] and metal–radical complexes.[6] In homometallic systems, spontaneous magnetization has been observed for complex compounds containing strongly anisotropic paramagnetic ions with high S values, such as Fe(II)[7] or Cr(II).[8] Ferromagnetism is also shown by electron transfer salts,[9] and V(TCNE)$_x$, a magnet with a T_c exceeding room temperature,[10] belongs to this family. Spin-canting is well documented for several Cu(II) compounds[11,12] (including the hydrated formate Cu(HCOO)$_2$·4H$_2$O) and also for the case of a ligand-induced strongly anisotropic Mn(II) compound.[13]

As far as we know, three structural modifications of the anhydrous copper formate compound have been reported,[14] but their chemical and/or structural relationships are not unambiguously established to date.[15–18] Whereas crystals of the α form are easily obtained from copper–formic acid solutions, the β form has been only isolated as polycrystalline samples through dehydration of Cu(HCOO)$_2$·4H$_2$O. The crystal structure of the α-[Cu(HCOO)$_2$] phase (usually named *royal blue*) has been

---

® Abstract published in *Advance ACS Abstracts,* August 15, 1993.

(1) *Magnetic Molecular Materials*; D. Gatteschi et al., Eds.; Kluwer Academic Publishers: Dordrecht: The Netherlands, 1991.
(2) Carlin, R. L. *Magnetochemistry*, Springer-Verlag: Berlin, 1985; p 142.
(3) Gadet, V.; Mallah, T.; Castro, I.; Verdaguer, M. *J. Am. Chem. Soc.* **1992,** *114,* 9213 and references therein.
(4) Lloret, F.; Nakatani, K.; Journaux, Y.; Kahn, O.; Pei, Y.; Renard, J. P. *J. Chem. Soc., Chem. Commun.* **1988,** 642.
(5) Nakatani, K.; Bergerat, P.; Codjovi, E.; Mathonière, C.; Pei, Y.; Kahn, O., *Inorg. Chem.* **1991,** *30,* 3978.
(6) Caneschi, A.; Gatteschi, D.; Renard, J. P.; Rey, P., Sessoli, R. *J. Am. Chem. Soc.* **1989,** *111,* 785.
(7) Martinez-Lorente, M. A.; Tuchagues, J. P.; Petrouleas, V.; Savariault, J. M.; Poinsot, R.; Drillon, M. *Inorg. Chem.* **1991,** *30,* 3587.
(8) Staulo, G.; Bellitto, C. *J. Mater. Chem.* **1991,** *1,* 915 and references therein.
(9) (a) Miller, J. S.; Calabrese, J. C.; Dixon, D. A.; Epstein, A. J.; Bigelow, R. W.; Zhang, J. H.; Reiff, W. M. *J. Am. Chem. Soc.* **1987,** *109,* 769. (b) Broderick, W. E.; Thomson, J. A.; Day, E. P.; Hoffman, B. M. *Science* **1990,** *249,* 410. (c) Yee, G. T.; Manriquez, J. M.; Dixon, D. A.; McLean, R. S.; Groski, D. M.; Flippen, R. B.; Narayan, K. S.; Epstein, A. J.; Miller, J. S. *Adv. Mater.* **1991,** *3,* 309.
(10) Manriquez, J. M.; Yee, G. T.; McLean, R. S.; Epstein, A. J.; Miller, J. S. *Science* **1991,** *252,* 1415.
(11) Bakalbassis, E.; Bergerat, P.; Kahn, O.; Jeannin, S.; Jeannin, Y.; Dromzee, Y.; Guillot, M. *Inorg. Chem.* **1992,** *31,* 625.
(12) De Jongh, L. J.; Miedema, A. R. *Experiments on Magnetic Model Systems*; Taylor and Francis Ltd.: London, 1974.
(13) Awaga, K.; Maruyama, Y. *Phys. Rev. B* **1991,** *44,* 2589.
(14) (a) Martin, R. L.; Waterman, H. *J. Chem. Soc.* **1959,** 1359. (b) Galwey, A. K.; Jamieson, D. M.; Brown, M. E. *J. Phys. Chem.* **1974,** *78,* 2664.
(15) Barclay, G. A.; Kennard, C. H. L. *J. Chem. Soc.* **1961,** 3289.
(16) Buerger, N.; Fuess, H. *Solid State Commun.* **1980,** *34,* 699.
(17) Günter, J. R. *J. Solid State Chem.* **1980,** *35,* 43.
(18) Heyns, A. M.; Range, K. J. *J. Mol. Struct.* **1987,** *57.*

0020-1669/93/1332-4337$04.00/0

Table I. Crystallographic Data for β-[Cu(HCOO)$_2$]

empirical formula	$C_2H_2CuO_4$	β, deg	122.14(2)
fw	151.52	V, Å^3	194.6(5)
cryst syst	monoclinic	Z	2
space group	$P2_1/a$, No. 14	ρ_{calcd} g·cm^{-3}	2.54
T	20 °C	λ(Mo Kα), Å	0.709 26
a, Å	8.187(2)	μ(Mo Kα), cm^{-1}	53.77
b, Å	7.922(2)	$R(F_o)^a$	0.044
c, Å	3.616(6)	$R_w(F_o)^b$	0.051

[a] $R = \sum|F_o| - |F_c|/\sum|F_o|$. [b] $R_w\|F_o| - |F_c\|^2/\sum w|F_c|^2]^{1/2}$.

determined by single-crystal X-ray diffraction methods.[15] Besides this, a structural model for the β-[Cu(HCOO)$_2$] phase (the *blue* modification) has been proposed taking as reference the crystal structure of the parent tetrahydrate[17] and assuming that the dehydration occurs topotactically. The existence of a third variety has been reported,[14] but it has not been well characterized.

With respect to the magnetic behavior of these compounds only preliminary studies on α-[Cu(HCOO)$_2$] have been reported, suggesting a ferromagnetic behavior with an ordering temperature of about 10 K, although neutron powder diffraction at liquid helium did not show the existence of magnetic ordering.[16]

In the present work we report the first direct synthesis, the crystal structure, and the magnetic characterization of one polymorph of the anhydrous copper(II) formate, the β-[Cu(HCOO)$_2$] phase, as well as the magnetic characterization of the α-[Cu(HCOO)$_2$] phase.

Experimental Section

Preparation of the Compounds. Both α and β polycrystalline anhydrous copper(II) formates were prepared as previously described in the literature.[14,15,17] Single crystals of the β phase of quality high enough for X-ray structural determination were isolated, for the first time, by a new route involving direct reaction between CuO (7.24 g, 0.091 mmol) and a formic acid (85%)–water (20:80) mixture (100 mL). By evaporation of the so-prepared solution at 85 ± 2 °C well-formed blue prismatic crystals result.

C and H contents in the solids were determined by elemental analysis, and Cu content was determined by atomic absorption using a Perkin-Elmer 300 AA spectrophotometer. In all analyzed samples, the C, H, and Cu contents correspond to the proposed molecular formula within the experimental error. Anal. Found (calcd) for α-[Cu(HCOO)$_2$]: Cu, 41.7 (41.4); C, 15.2 (15.6); H, 1.5 (1.3). Anal. Found (calcd) for β-[Cu(HCOO)$_2$]: Cu, 41.1 (41.4); C, 15.5 (15.6); H, 1.4 (1.3).

Crystal Structure Determination of β-[Cu(HCOO)$_2$]. Single-crystal X-ray data were recorded using a CAD-4 Enraf-Nonius diffractometer. Lattice parameters were obtained by the centering of 25 strong reflections with 2θ angles higher than 13°. The intensity of three standard reflections, measured every hour, was monitored throughout the data collection, and no significant variation was detected. Lorentz, polarization and absorption (empirical)[19] corrections were applied. Other important features of the data collection are summarized in Table I.

Data collection showed systematic absences consistent with the space group $P2_1/a$, as previously pointed by Günter[17] from powder diffraction data. The structure was solved by direct methods and refined with the SHELX76[20] system by weighted anisotropic full-matrix least-squares methods. After refinement of positional and anisotropic thermal parameters for all non-hydrogen atoms, the position of the hydrogen atom was calculated and its isotropic thermal parameter refined in the last cycle, leading to a final value of R (R_w) of 0.044 (0.051). The residual maximum in the final difference map was a peak of 0.3 e Å^{-3} located near the copper atom. Scattering factors and corrections for anomalous dispersion were taken from ref 21. The geometrical calculations were performed with XANADU[22] and molecular drawings were made by using ORTEP.[23] The final atomic coordinates are given in Table II and selected bond distances and angles in Table III.

Table II. Positional Parameters and Their Estimated Standard Deviations (in Parentheses) for β-[Cu(HCOO)$_2$]

atom	x/a	y/b	z/c	B_{eq},^{a} Å^2
Cu	0	0	0	1.21(3)
C	0.2597(3)	0.2638(2)	0.0857(9)	1.15(8)
O(1)	0.1718(2)	−0.0895(2)	−0.1757(4)	1.68(6)
O(2)	0.1284(2)	0.2186(2)	0.1401(5)	2.01(7)

[a] $B_{eq} = 8\pi^2(U_{11} + U_{22} + U_{33})/3$.

Table III. Selected Bond Distances (Å) and Angles (deg) with Estimated Standard Eviations in Parentheses for β-[Cu(HCOO)$_{12}$]^a

Cu Coordination Sphere			
Cu–O(1)	1.958(1)	Cu–O(2)	1.948(2)
Cu–O(1)^{ii}	2.628(2)		
O(2)–Cu–O(2)^i	180.0(0)	O(1)–Cu–O()^i	180.0(0)
O(1)–Cu–O(2)	91.4(1)	O(1)–Cu–O(1)^i	86.4(1)
O(1)–Cu–O(1)^{ii}	103.1(1)	O(2)–Cu–O(1)^{ii}	93.2(2)
O(1)^i–Cu–O(1)^{ii}	76.9(1)	O(2)^i–Cu–O(1)^{ii}	86.8(1)
Carboxylate Group			
C–O(1)	1.256(2)	C–O(2)	1.245(2)
O(1)–C–O(2)	122.0(3)		

[a] The angles between the second axial atom O(1)^{iii} and the equatorial oxygen atoms are the complementary of the O(2)^{ii}–Cu–O$_{eq}$ ones. Symmetry operations: (i) $-x, -y, -z$; (ii) $x, y, 1 + z$; (iii) $-x, -y, 1 - z$.

Physical Measurements. X-ray powder diffraction patterns were obtained by means of a Rigaku CD 2455D 6 diffractometer using Cu Kα radiation.

Ac magnetic susceptibility measurements, $\chi = \chi' - i\chi''$, were carried out on polycrystalline samples, in the temperature range 4.2–300 K, using a Lake Shore Cryotonics Inc. Model 7000 AC equipment at zero dc field. The frequency and exciting field amplitudes used were 333.3 Hz and 0.1, 1, and 10 Oe. The dc magnetic susceptibility and magnetization measurements were carried out on polycrystalline samples with a pendulum-type apparatus equipped with a helium cryostat. The experimental susceptibilities were corrected both for the diamagnetic contributions and the TIP of the Cu(II) ion, estimated to be 60 × 10^{-6} emu and mol^{-1} per Cu(II) ion.[24]

Polycrystalline powder EPR spectra were recorded on a Bruker ER 200 D spectrometer (equipped with a low temperature device) working at X-band (9.4–9.7 GHz). Magnetically modulated microwave absorption (MAMMA)[25] of samples of about 10–15 mg was measured by means of this spectrometer with a modulation frequency of 100 kHz, modulation amplitude of 5 G, microwave power of 2 mW, and application of a dc continuous magnetic field of 100 G.

Results and Discussion

Synthesis. In the course of our studies on the Sr–Cu(II)–HCOOH–H$_2$O system, besides the SrCu(HCOO)$_4$ phase (isostructural to CaCu(HCOO)$_4$, recently reported as being a new one-dimensional ferromagnetic bis(μ-oxo ligand)-bridged chain compound[26]), other crystalline phases appeared. These last species were identified by means of X-ray powder diffraction measurements as α-[Cu(HCOO)$_2$] and β-[Cu(HCOO)$_2$]. MAMMA measurements (see below) on those polyphasic samples revealed two independent absorption peaks near 10 and 30 K, which suggested the presence of two 3d magnetic phase transitions at these temperatures. The ac magnetic susceptibility experiments confirmed these results indicating a probable ferromagnetic character of both ordered phases below 30.4 and 8.2 K,

---

(19) North, A. C. T.; Phillips, D. C.; Mathews, F. S. *Acta Crystallogr.* **1968**, *A24*, 351.

(20) Sheldrick, G. M. SHELX 76. Program for Crystal Structure Determination. University of Cambridge, Cambridge, England, 1976.

(21) *International Tables for X-ray Crystallography*, Ibers, J. A., Hamilton, W. C., Eds.; Kynoch Press: Birmingham, England, 1974; Vol. 4.

(22) Roberst; P.; Sheldrick, G. M. XANADU. Program for Crystallographic Calculations. University of Cambridge, Cambridge, England, 1975.

(23) Johnson, C. K. *ORTEP*; Report ORNL-3794; Oak Ridge National Laboratory: Oak Ridge, TN, 1965.

(24) Earnshaw, A. *Introduction to Magnetochemistry*; Academic Press: London and New York, 1968.

(25) (a) Kim, B.; Bohandy, J.; Moorjandi, K.; Adrian, F. J.; *J. Appl. Phys.* **1988**, *63*, 2029. (b) Glarum, S. H.; Schneemeyer, L. F.; Wszcak, J. V. *Phys. Rev. B* **1990**, *41*, 1837. (c) Shaltiel, D.; Bill, H., Grayevsky, A.; Jundd, A.; Lovy, D.; Sadowski, W.; Walker, E. *Phys. Rev. B* **1991**, *43*, 1359.

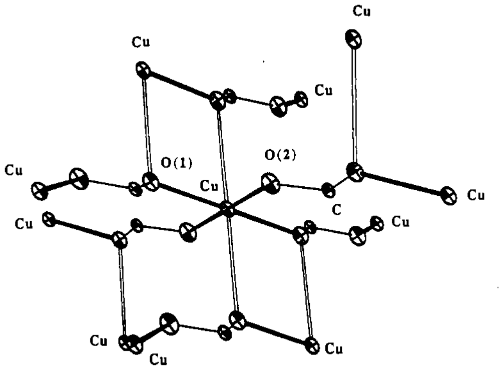

Figure 1. Perspective view and atomic numbering in the β-[Cu(HCOO)$_2$] phase showing the connectivity between the copper atoms.

respectively. Previously reported results on the α phase[14,16] suggested a ferromagnetic behavior with T$_c$ near 10 K. Therefore, it initially seems reasonable to associate the lower temperature transition to the α phase and then conclude that the β polymorph behaves like a ferromagnet with an ordering temperature around 30 K. An independent and deeper study of each of two copper formate polymorphs should be then significant.

The synthesis of α-[Cu(HCOO)$_2$] is straightforward and its crystal structure has been previously reported.[14] So, we focused our interest on the obtaining of single crystals of β-[Cu(HCOO)$_2$]. In attempts to grown single crystals suitable for a X-ray study of the β phase, a series of aqueous solutions with variable [HCOOH$_{(aq)}$]/[Cu$^{2+}{}_{(aq)}$] ratio (from 2 to 8) was prepared and treated at temperatures ranging from 60 to 90 °C. In most cases, within a few hours, blue crystalline solids were obtained and their X-ray diffraction pattern showed that both α and β phases were present. Notwithstanding, those preparations carried out in the narrow temperature range of 85 ± 2 °C (see Experimental Section) lead to the obtaining of monophasic β-[Cu(HCOO)$_2$] samples, as was confirmed by powder X-ray diffraction.

We have also observed that the β → α solid-state phase transition not only takes place at *high* temperature (100 °C) as has been previously reported[18] but it also occurs at room temperature (22 ± 3 °C), although very slowly. Thus, whereas well-developed crystals of the β phase took several months for their complete transformation into the α form, powdered samples transform in a few weeks. Consequently, all the characterization experiences on that phase were performed on *freshly* prepared (and low-temperature stored) pure samples.

Crystal Structure of the β-[Cu(HCOO)$_2$)] Phase. The coordination polyhedron around copper atoms—which lie on symmetry centers (*2a* sites)—can be described as tetragonally elongated octahedron (CuO$_4$O′$_2$ chromophore). The equatorial plane involves four oxygen atoms from four different formate groups nearly coplanar to the central metal (Figure 1). The Cu–O′$_{ax}$ distance exceeds the Cu–O$_{eq}$ ones (see Table II) by more than 0.67 Å. Then, according to Hathaway's criterion,[27] the axial oxygen atoms must be considered as semicoordinated. In fact, the tetragonality parameter[28] ($T = 0.72$) is significantly smaller than those observed in different [CuO$_6$] polyhedra found in related compounds (*i.e.*, in the well-characterized alkaline earth–copper(II) formates,[26,28,29] or the copper(II) hydrated formates,[30] where the T parameter ranges from 0.8 to 0.9), which indicates a more pronounced tetragonal distortion in this compound.

Each carboxylate group connects three copper atoms and shows a structural conformation *a*–3–*as*.[31] They are slightly asymmetric, with a small value of the asymmetric parameter δ ($\delta = (d_{[C-O(1)]} - d_{[C-O(2)]}) \times 10^{-3} = 11$), which is consistent with the expected charge density polarization in the COO group. As expected, the longer C–O distance corresponds to the oxygen atom which acts as bidentate (O(1)).

Each copper atom is connected to two copper atoms through bis(μ-oxo–carboxylate) bridges, defining infinite chains of edge-sharing [CuO$_6$] elongated octahedra, running parallel to the [001] axis. According to Willett's notation,[32] the stacking of [CuO$_6$] units through bis(μ-oxo ligand) bridges is of the type I (1 ($^1/_2$, $^1/_2$) pattern). Although this type of bridge topology between copper atoms is common among bis(μ-ligand)-bridged compounds, the only examples known to date in which both bridging atoms are oxygen atoms from carboxylate groups are the α-[Cu(HCOO)$_2$] phase[15] and the MCu(HCOO)$_4$ (M = Ca, Sr) and Ca$_2$Cu(HCOO)$_6$ mixed formates.[26] In these bimetallic formates there exist well isolated bis(μ-oxo ligand)-bridged chains, although the stacking of [CuO$_6$] units through the bridges is of type II in Willett's notation.[32]

The connectivity between copper atoms belonging to different chains is a relevant structural feature. So, each copper atom in a chain is connected to eight copper atoms of four different adjacent chains through six carboxylate groups (see Figure 1). Four of these neighboring copper atoms are to the central atom being connected to it *via* four carboxylate groups (lying also in the same plane) with an *anti–anti* structural function. This fact gives rise to a layer network parallel to (001) similar to that observed in the Cu(HCOO)$_2$·4H$_2$O compound.[33] Connection to the other four copper atoms is established *via* carboxylate bridges having an *anti–syn* structural function.

Structural Relationships and Phase Transition Mechanism. The structure of the α-[Cu(HCOO)$_2$] compound can formally be described as built up of dimeric entities formed by two edge-sharing CuO$_4$O′ polyhedra, giving rise to bis(μ-oxo) [Cu$_2$O$_8$] entities. Moreover each bis(μ-oxo) [Cu$_2$O$_8$] unit is connected to their neighboring dimeric units through carboxylate groups, so an infinite three-dimensional array results. Cu(II) atoms are in a 4 + 1 environment of square pyramidal geometry. The basal coordination positions are occupied by four oxygen atoms belonging to four different formate groups with the metal atom in the plane (the displacement of 0.003 Å is within the experimental error). The apical position is occupied by an oxygen atom belonging to the basal plane of the other Cu(II) ion in the bis(μ-oxo) [Cu$_2$O$_8$] unit. The Cu–O$_{ax}$ distance (2.410 Å) is longer that the Cu–O$_{eq}$ one (mean value of 1.967 Å). As was discussed by Buerger,[16] a second Cu–O″$_{ax}$ interaction might be considered, where the O″$_{ax}$ atom belongs to an adjacent bis(μ-oxo) [Cu$_2$O$_8$] unit. Nevertheless, the very long Cu–O″ distance (2.79 Å) and the small O′–Cu–O″ angle (126.8°) suggest that it should be a very weak interaction and, consequently, may be ignored.

On the other hand, unlike what has been found in the β phase, in the α phase there are two crystallographically different carboxylate groups. One of them (*a–2–s* type) links copper atoms along the [010] directions, and the other (nearly *a–3–sa* type) links them along the [100] direction.

---

(26) Sanchis, M. J.; Gómez-Romero, P.; Folgado, J. V.; Sapiña, F.; Ibañez, R.; Beltrán, A.; García, J.; Beltrán, D. *Inorg. Chem.* **1992**, *31*, 2915.

(27) Hathaway, B. J. In *Comprehensive Coordination Chemistry*; Wilkinson, G., Ed.; Pergamon: Oxford, England 1985; Vol. 5, p 604.

(28) (a) Fitgerald, W.; Foley, J.; McSweeney, D.; Ray, N.; Shenhan, D.; Tyagi, S.; Hathaway, B. J., O'Brien, P. *J. Chem. Soc., Dalton Trans.* **1982**, 1117. (b) Hathaway, B. J. *Struct. Bonding* **1984**, *57*, 55 and references therein.

(29) (a) Rao, R. V. G. S.; Sundarama, K.; Rao, G. S., *Z. Kristallogr.* **1958**, *110*, 231. (b) Baggio, R. F.; de Perezzo, P. K.; Polla, G. *Acta Crystallogr.* **1985**, *41C*, 194.

(30) (a) Bukowska-Strzyzewska, Kay, M. J.; Almodovar, I.; Kaplan, S. F. *Acta Crystallogr.* **1965**, *19*, 357. (b) Kay, M. J.; Almodovar, I.; Kaplan, S. F. *Acta Crystallogr.* **1968**, *B24*, 482.

(31) Porai-Koshits, M. A. *Zh. Strukt. Khim.* **1980**, *21*, 146.

(32) Geiser, U.; Willett, R. D.; Lindbeck, M.; Emerson, K. *J. Am. Chem. Soc.* **1986**, *108*, 1173.

(33) (a) Kiriyama, R.; Ibamoto, H.; Matsuo, K. *Acta Crystallogr.* **1954**, *7*, 482. (b) Okada, K.; Kay, M. I.; Kromer, D. T.; Almodovar, I. *J. Chem. Phys.* **1966**, *44*, 1648.

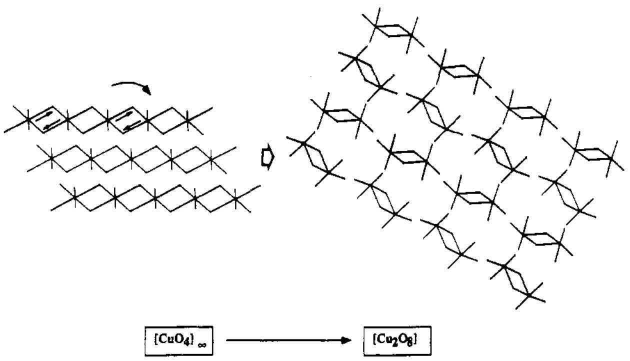

Figure 2. Possible mechanistic scheme for the β-$[Cu(HCOO)_2]$ → α-$[Cu(HCOO)_2]$ transformation.

According to the structural information, it may be suggested an explanation of how the β → α transformation takes place. The proposed model assumes that the bis(μ-oxo) $[Cu_2O_8]$ dimeric entities present in the α form stem from the ***breaking*** of the bis(μ-oxo) $[CuO_4]_\infty$ chains in the β one (Figure 2). In this sense, we have already mentioned above that the out-of-plane copper–oxygen interactions are weak (such a consideration is also supported by vibrational spectroscopic studies on this phase[18]). Thus, the transformation from the β to the α phase might be thought of to occur by a chain dimerization (the shortest Cu–Cu distance in the β form is 3.62 Å and decreases to 3.44 Å in the α one), in conjunction with a relative rotation of the *incipient* bis(μ-oxo-ligand) $[Cu_2O_8]$ entities (which implies, in fact, the breaking of the chains).

Finally, significant structural differences between both polymorphs may be outlined if we pay attention to the arrangement of $[CuO(eq)_4]$ and $[CO_2]$ units. In the β phase these units are nearly coplanar, leading to a well-defined layer network. However, if a remembrance of this layered arrangement is looked for in the α-phase, it can be observed that the planarity has been lost (so, the dihedral angles between connected $[CuO(eq)_4]$ units range from 78 to 117° and from 11 to 136° between the $[CuO(eq)_4]$ units and the $[CO_2]$ ones) and a *warped-layer* network results. This fact, besides the different structural function of the carboxylate groups, will be invoked afterward in the discussion of the magnetic behavior.

Bearing in mind all these considerations, it may be stated that the polymorphic transformation from the metastable β-$[Cu(HCOO)_2]$ phase to the stable α-$[Cu(HCOO)_2]$ phase is, from a structural point of view, essentially distortional, since the breaking of the bis(μ-oxo ligand) $[CuO_4]_\infty$ chains only requires (from a formal point of view) the breakdown of one relatively weak copper–oxygen ($Cu–O_{ax}$) bond per copper atom.

Magnetic Properties. ***α-[Cu(HCOO)₂] Phase.*** Figure 3 shows the thermal behavior of the in-phase component of the ac susceptibility, χ', for the α-$[Cu(HCOO)_2]$ phase, measured with an ac excitation field of 1 Oe. In order to cover the 3 orders of magnitude of χ', a semilogarithmic plot has been used. The most relevant features of this curve are the presence of a sharp peak at $T_p = 8.0 \pm 0.2$ K, and the temperature dependence of χ'. This last slowly increases upon cooling down and, close to T_p, suddenly goes up and becomes almost divergent. The χ' value in the maximum is 22.25 emu mol^{-1}, which is practically 400 times greater than that expected for an uncoupled system of copper(II) ions. The value of the product $\chi'T$ for the maximum is 178.42 emu K mol^{-1}.

In the inset of Figure 3 both components of the ac susceptibility (the in-phase, χ', and the out-of-phase, χ'') have been represented using an enlarged linear scale. The absorption, χ'', is zero above T_p. Close to this temperature it increases sharply to reach its maximum value, about one-tenth of χ', and then it decreases slowly on cooling down. This behavior clearly indicates that the system undergoes a phase transition from a paramagnetic to a long-range order magnetic state with a ferromagnetic component.

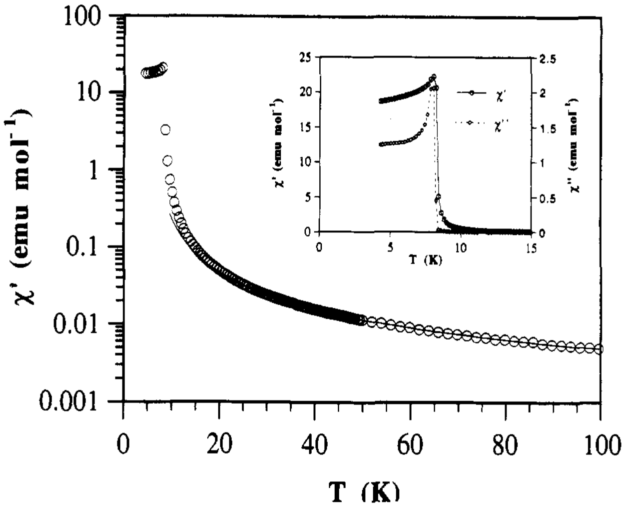

Figure 3. Semilogarithmic plot of the thermal variation of the in-phase component of the ac susceptibility $\chi'(T)$ of α-$[Cu(HCOO)_2]$. In the inset, both components of the ac susceptibility, $\chi'(T)$ and $\chi''(T)$, have been represented in the neighborhood of T_c using an enlarged lineal scale.

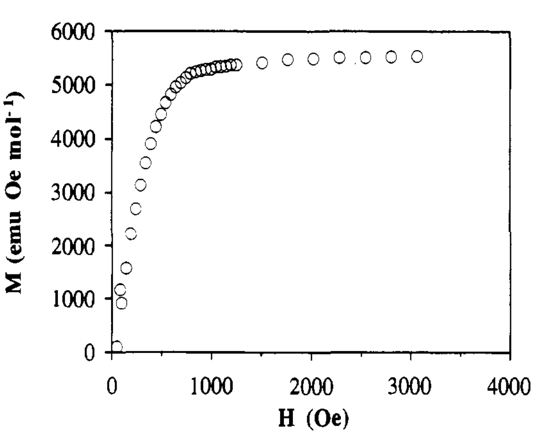

Figure 4. Magnetization measurements of α-$[Cu(HCOO)_2]$ at $T = 5.8$ K, increasing the magnetic field.

A pronounced dependence of the susceptibility signals (χ' and χ'') with the excitation field is observed below T_p. In the case of χ', this dependence is reflected not only in the magnitude of the signal, which increases concomitantly with the excitation field, but also in the position of the maximum, which moves to lower temperatures as the excitation field increases. Thus, the critical temperature for the transition, determined from the measurements performed with the lowest excitation field (0.1 Oe), is observed to be $T_c = 8.2 \pm 0.2$ K.

The thermal variation of the inverse of the in-phase component of the ac susceptibility, χ', follows the Curie–Weiss law above ca. 25 K with Curie and Weiss constants of $C = 0.404$ emu K mol^{-1} and $\Theta = 13.1$ K. The estimated value of the Landé factor, g(2.08), is typical of a Cu(II) ion. The positive value of Θ indicates that ferromagnetic interactions dominate above the order temperature.

To clarify the nature of the magnetic ordered state, we have measured the isothermal magnetization $M(T,H)$ at 5.8 K with fields up to 3000 Oe. The results have been represented in Figure 4. For fields higher than 800 Oe the magnetic moment is saturated, and $M(T,H)$ changes linearly with the field, with a slope $dM/dH = 0.033$ emu mol^{-1}. A linear extrapolation between 2000 and 3000 Oe allows us to derive the net magnetization per Cu ion, 5439.5 emu Oe mol^{-1}. So, the net magnetic moment per Cu ion in the direction of the magnetization is 1.68, μ_B, clearly indicating the ferromagnetic nature of the ordered state.

Table IV. Magnetic Atom Numbering and Definition of Magnetic Modes for the α-[Cu(HCOO)]$_2$ Phase

Atomic Numbering

Cu(1)	x, y, z	Cu(5)	$-x, -y, -z$
Cu(2)	$^1/_2 + x, {}^1/_2 - y, -z$	Cu(6)	$^1/_2 - x, {}^1/_2 + y, z$
Cu(3)	$-x, {}^1/_2 + y, {}^1/_2 - z$	Cu(7)	$x, {}^1/_2 - y, {}^1/_2 + z$
Cu(4)	$^1/_2 - x, -y, {}^1/_2 + z$	Cu(8)	$^1/_2 + x, y, {}^1/_2 - z$

Magnetic Modes

$F_1 = S_1 + S_2 + S_3 + S_4$	$F_2 = S_5 + S_6 + S_7 + S_8$
$G_1 = S_1 - S_2 + S_3 - S_4$	$G_2 = S_5 - S_6 + S_7 - S_8$
$C_1 = S_1 + S_2 - S_3 - S_4$	$C_2 = S_5 + S_6 - S_7 - S_8$
$A_1 = S_1 - S_2 - S_3 + S_4$	$A_2 = S_5 - S_6 - S_7 + S_8$
$F^+ = F_1 + F_2$	$F^- = F_1 - F_2$
$G^+ = G_1 + G_2$	$G^- = G_1 - G_2$
$C^+ = C_1 + C_2$	$C^- = C_1 - C_2$
$A^+ = A_1 + A_2$	$A^- = A_1 - A_2$

Table V. One-Dimensional Representations for **k** = [0,0,0] of Space Group *Pbca* and Basis Functions Corresponding to Magnetic Atoms Situated on General Positions (8*c*), Where the + and – Symbols Correspond to the Characters +1 and –1 of the Generators 2_{1x}, 2_{1y}, –1

	x	y	z		x	y	z
Γ_{1g} (+ + +)	C^+_x	G^+_y	A^+_z	Γ_{1u} (+ + –)	C^-_x	G^-_y	A^-_z
Γ_{2g}(– + +)	A^+_x	F^+_y	C^+_z	Γ_{2u} (– + –)	A^-_x	F^-_y	C^-_z
Γ_{3g} (+ – +)	F^+_x	A^+_y	G^+_z	Γ_{3u}(+ – –)	F^-_x	A^-_y	G^-_z
Γ_{4g} (– – +)	G^+_x	C^+_y	F^+_z	Γ_{4u}(– – –)	G^-_x	C^-_y	F^-_z

A condition for the existence of ferromagnetism or weak ferromagnetism is that nuclear and magnetic cells must be identical and, in this case, the reduced propagation vector of the magnetic structure can be taken as **k** = [0, 0, 0]. The application of the Macroscopic Theory of Bertaut[34] to explore the possible magnetic structures of this phase is straightforward. The numeration of the magnetic atoms, as well as the form of the magnetic modes are given in Table IV. The generators of the space group *Pbca* are (2_{1x}, 2_{1y}, –1), where the notation stands for the binary axis along **a** and **b** and the inversion center at the origin, respectively. The one-dimensional representations of *Pbca* for **k** = [0, 0, 0] can be labeled by the characters corresponding to the generators. In Table V, we give the invariant spin configurations which transform according the eight representations of *Pbca*. As it can be seen, the ferromagnetic modes F_i^+ ($i = x, y, z$) transform as different irreducible representations. So, the observed magnetic behavior must correspond only to one ferromagnetic mode.

The magnetic lattice of this compound is complicated, and it consists of three different exchange pathways between copper atoms, giving rise to three in equivalent exchange integrals. Each copper atom is connected to one copper atom within a dimer and four other copper atoms belonging to other dimers, in such a way that each dimer is connected to eight other dimers. These four exchange pathways are equivalent two by two by symmetry reasons.

J_d describes the intradimer interaction. Each copper atom is connected with another copper atom through a bis(μ-oxo-carboxylate) bridge. The other exchange integrals, J_1 and J_2, represents interdimer exchange pathways, involving *a-2-s* carboxylate bridges, and define a 2d square planar lattice of copper atoms. In this description, the intradimer exchange pathway represents the interlayer one. Assuming, at a first approximation, that the intradimer exchange integral, J_d, is lower than the interdimer ones, J_1 and J_2, and assuming also that $J_1 = J_2$, the magnetic behavior of this compound can be described by the series of expansion for 2d square planar, $S = {}^1/_2$ ferromagnetic Heisenberg model.[35] In the range 20–100 K (solid line in Figure 3) the best fit is obtained with the following set of parameters: $g = 2.07$ and $J/k = 4.3$ K.

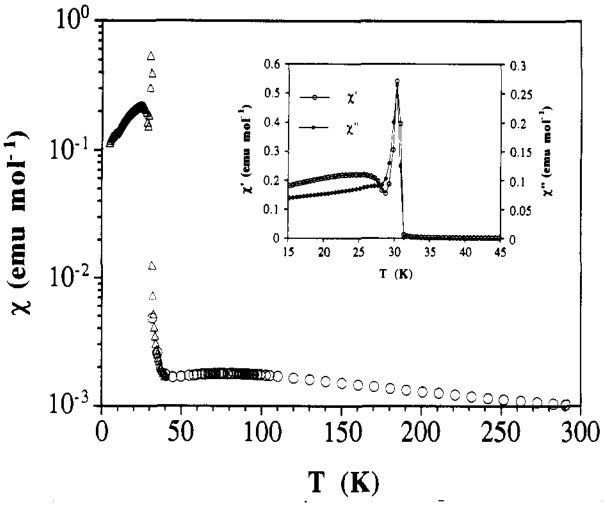

Figure 5. Semilogarithmic plot of the thermal variation of the susceptibility of β-[Cu(HCOO)$_2$]: (△) in-phase component of the ac susceptibility; (○) dc susceptibility. In the inset, both components of the ac susceptibility, $\chi'(T)$ and $\chi''(T)$, have been represented in the neighborhood of T_c using an enlarged lineal scale.

It is possible also estimate the interlayer exchange integral J_d extending the analysis of the magnetic properties at temperatures lower than 20 K by means of a molecular field correction term in the expression of the susceptibility calculated from the series of expansion for 2d square planar, $S = {}^1/_2$ ferromagnetic Heisenberg model. The best estimation for the intradimer exchange integral, obtained from the best fit of the magnetic data between 10 and 100 K, is $J_d/k = 0.38$ K.

The exchange integral J can be expressed as a sum of both ferromagnetic (J_F) and antiferromagnetic (J_{AF}) contributions, $J = J_F + J_{AF}$.[36] Whereas the ferromagnetic contribution is usually small, the antiferromagnetic one is proportional to the square of the overlap integral between magnetic orbitals.[37] So, the resulting sign of the exchange integrals will depend, on a great extent, on the amplitude of the overlap between magnetic orbitals, which are built up from the spin-carrying orbitals of the copper atoms ($d_{x^2-y^2}$ orbitals) and the adapted linear combinations of the orbitals of the bridging groups. Referring to the intralayer exchange interaction, as far as the oxygen atoms of the carboxylate bridges belongs to the equatorial planes of the copper atoms, the resulting signs of the exchange integrals are likely to be related to the role played by the exchange propagating orbitals of the bridging COO groups. This role is far from being well understood, except in few defined orientations of the bridging COO group with respect to the equatorial planes of both copper coordination polyhedra, and is currently under study.[38] With respect to the interlayer (intradimer) exchange interaction, it is evident that the magnetic orbitals are mismatched with respect to interaction between them *via* formate orbitals. Departures from the idealized symmetry would allow some admixture with the d_{z^2} orbital but, in any case, the overlap would be very poor, and $J_{AF} \approx 0$.

β-[Cu(HCOO)$_2$]. Figure 5 shows the thermal behavior of the susceptibility of a powdered sample of β-[Cu(HCOO)$_2$] phase. The data at low temperatures (△) are the in-phase component, χ', of the ac susceptibility, measured with an exciting field of 1 Oe and a excitation frequency of 333.3 Hz in a zero external dc magnetic field. The data at high temperatures (○) were measured

---

[34] Bertaut, E. F. In *Magnetism*; Rado, G. T., Suhl, H., Eds.; Academic Press: New York 1963; Vol. 3 p. 149.

[35] Navarro, R. In *Magnetic Properties of Layered Transition Metal Compounds*; de Jongh, L. J. Editor, Kluwer Academic Publishers: Dordrecht, The Netherlands, 1990; pp 105–190.

[36] Girerd, J. J.; Journaux, Y.; Kahn, O. *Mol. Phys.* **1977**, *34*, 1063.

[37] Kahn, O. *Angew. Chem.*, **1985**, *24*, 834.

[38] Alvarez, S.; Lloret, F. Work in progress.

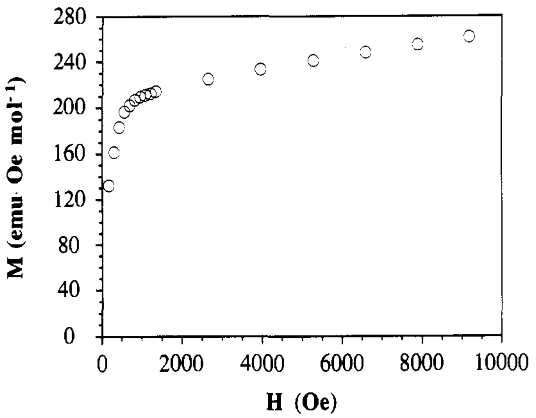

Figure 6. Magnetization measurements of β-[Cu(HCOO)$_2$] at T = 5.8 K, increasing the magnetic field.

with a pendulum type equipment, using a field strength of 15 KOe. Both sets of data are seen to agree quite well. In this case, the behavior is more complicated than that observed for the α-[Cu(HCOO)$_2$] phase. As it can be noted, upon cooling down, the susceptibility shows a broad maximum at T_{max} = 76.6 K ($\chi_{max} = 1.79 \times 10^{-3}$ emu mol^{-1}). At lower temperatures, χ' slowly decreases, reaching a minimum, and then increases. At *ca.* 31.5 K, it suddenly increases and becomes almost divergent at a temperature $T_c = (30.4 \pm 0.2)$ K (χ_{max} = 0.55 emu mol^{-1}). Upon further cooling, another anomaly is observed, displaying another broad maximum at a temperature $T_k = (24.6 \pm 0.5)$ K, i.e., 6.2 K lower than the previous one.

In the inset of Figure 5 both components of the ac susceptibility, χ', and the out of phase component, χ'', have been represented using an enlarged linear scale around the peak at T_c. The absorption, χ'', is zero down to T_c and, at this temperature, increases sharply and takes its highest value (about half of χ'), decreasing then on cooling down. This behavior clearly indicates that the system undergoes a magnetic phase transition at T_c to an ordered state with a weak ferromagnetic component.

A marked field dependence of the susceptibility signals below T_c is observed. This dependence is now reflected in the magnitude of the signal at T_c, which increases with the excitation field, but contrary to the above case, there is no variation in the position of this peak (at least, within the excitation field amplitudes available with our equipment). On the other hand, the field dependence is also observed for the second anomaly, affecting both the magnitude of the signal and the position of this low-temperature broad maximum. All this phenomenology in the ac susceptibility below T_c in weak ferromagnets is attributed to domain wall motion.[39]

To clarify the nature of the magnetic ordered state, we have measured the isothermal magnetization $M(T,H)$ at 5.8 K with fields up to 10000 Oe. The results have been represented in Figure 6. For fields higher than 1000 Oe the magnetic moment is saturated, and $M(T,H)$ changes linearly with the field, with slope dM/dH = 0.0054 emu mol^{-1}. A linear extrapolation between 4000 and 10000 Oe allows us to derive the net magnetization for Cu ion, 212.6 emu Oe mol^{-1}. So the net magnetic moment per Cu ion in the direction of the magnetization is 0.0657 μ_B, clearly indicating the weak ferromagnetic nature of the ordered state. The canting angle is estimated to be greater than 2.2°.

The application to the Macroscopic Theory of Bertaut[34] also shows in this case the compatibility between crystal structure and weak ferromagnetism. The numeration of the magnetic atoms, as well as the form of the magnetic modes are given in Table VI. The generators of the space group $P2_1/a$ are (2_{1y}, -1) where the notation stands for the binary axis along **b** and the inversion center at the origin, respectively. The one-dimensional representations of $P2_1/a$ at **k** = [0, 0, 0] can be labeled by the characters corresponding to the generators. As the spin configuration is invariant under the inversion center, only the even (gerade) representations are relevant. Therefore, only the first generator is needed to label the representations. In Table VII we give the invariant spin configurations which transform according to the two even representations of $P2_1/a$ at **k** = [0, 0, 0] for a magnetic atom occupying an special position (2*a*) (point group symmetry -1). The observed magnetic behavior must correspond only to one ferromagnetic mode.

Table VI. Magnetic Atom Numbering and Definition of Magnetic Modes for the β-[Cu(HCOO)]$_2$ Phase

Atomic Numbering			
Cu(1)	0, 0, 0	Cu(2)	$^1/_2$, $^1/_2$, 0
Magnetic Modes			
$F = S_1 + S_2$		$A = S_1 - S_2$	

Table VII. Even One-Dimensional Representations for **k** = [0,0,0] of Space Group $P2_1/a$ and Basis Functions Corresponding to Magnetic Atoms Situated on Special Positions (2*a*), Where the + and − Symbols Correspond to the Characters +1 and −1 of the Generator 2_{1y}

	y	xz
$\Gamma_{1g}(+)$	F_y	A_{xz}
$\Gamma_{2g}(-)$	A_y	F_{xz}

The magnetic lattice of this compound consists of three different exchange pathways between copper atoms, giving rise to three inequivalent exchange integrals. J describes the intralayer interaction. Each copper atom has four copper atoms as its nearest neighbors in the layers, being connected to each other through one carboxylate bridge (whose structural type, considering only these two copper atoms, is *anti*). This interaction defines a 2d square planar lattice, and it is expected to be antiferromagnetic (see below). J_z describes the interlayer interaction in the chain direction. Each copper atom has two copper atoms as nearest neighbors, being connected through the bis(μ-oxo-carboxylate) bridge. This interaction is expected to be weak and could be expected to be ferromagnetic, on the basis of the magnetic behavior of the bimetallic calcium copper formates CaCu(HCOO)$_4$ and Ca$_2$Cu(HCOO)$_6$.[26] Finally, J' describes the interlayer interaction out of the chain direction. Each copper atom is connected to four other copper atoms of adjacent chains on adjacent layers through four carboxylate bridges (whose structural type, considering only these two copper atoms, is *anti–syn*). This interaction is expected to be very weak, due to the relative orientation of the magnetic orbitals with respect the carboxylate group (see below), and has been neglected in this analysis. These assumptions are confirmed by the observed magnetic behavior at temperatures above 50 K, which show the main feature of a 2d isotropic antiferromagnetic, namely a broad maximum well above the order temperature.

So, taking into account the crystal structure of this compound, the magnetic behavior at temperatures above ordering temperatures may be described by the series of expansion for the 2d square planar, $S = {}^1/_2$ antiferromagnetic Heisenberg model.[35] The best fit, between 60 and 300 K (solid line in Figure 7), is obtained with the following set of parameters: g = 2.05 and J/k = −41.4 K. The position and height for the antiferromagnetic χ maximum are well reproduced with these values[35] (theoretical values: T_{max} = 77.65 K; $\chi_{max} \approx 1.785 \times 10^{-4}$ emu mol^{-1}).

The interaction along the chain direction may be obtained from a molecular field type argument.[40] The 3d order temperature T_c for a system of weakly coupled layers is related with the correlation length in the layer ϵ_{2d}, evaluated at T_c, by

$$kT_c = (\epsilon_{2d})^2|J_z|S(S+1)$$

The correlation length for a 2d square planar Heisenberg model

---

[39] Groenendijk, H. A. Ph.D. Thesis, University of Leiden, 1981.

is [41]

$$\epsilon_{2d} = \exp(2|J|S(S + 1)/kT)$$

Then it is straightforward to obtain the interaction along the chain, in absolute value. The value of $|J_z|/k$ is observed to be 0.64 K.

We can use the Microscopic Theory of Bertaut[34] to explore the magnetic phase diagram for this magnetic lattice topology in the $J - J_z$ plane, using the stability conditions of the different possible collinear magnetic structures, in order to obtain information on the sign of the J_z exchange integral. The results of this analysis shows that crystal and magnetic structures are identical for $J_z > 0$. If $J_z < 0$, the magnetic cell is doubled in the c axis ($k_z = {}^1/_2$). Finally, for $J_z > 0$, mode A is stable for $J < 0$, whereas mode F is stable for $J > 0$. So, the results of this analysis are compatible with the value of J obtained from the analysis of the magnetic behavior above the order temperature and shows that the existence of weak ferromagnetism in this compound is only compatible with the crystal structure for a ferromagnetic interaction along the chain.

The resulting sign of the two different magnetic interactions depends, as has been previously discussed, on the amplitude of the overlap between magnetic orbitals.[36,37] The ground state of Cu(II) is adequately described by the $d_{x^2-y^2}$ orbital, given the local coordination of oxygen atoms around it. In the light of the structural features of this compound, this is one of the few cases in which the role played by the orbital of the COO group is clear. The exchange interaction in the layer, J, should be antiferromagnetic, due both to the relative orientation of the $d_{x^2-y^2}$ orbitals on neighboring Cu(II) ions and to the structural function and orientation (parallel to the equatorial plane of the coordination) polyhedron) of the carboxylate bridge. This orientation allows a good overlap between the magnetic orbitals via σ orbitals of the COO group. With respect to the exchange interaction between layers (in the bis(μ-oxo ligand)-bridged CuO_4 chains), it is evident that the magnetic orbitals are mismatched to interact between them *via* formate orbitals. Departures from the idealized symmetry would allow some admixture with the d_{z^2} orbital, but in any case, the overlap would be very poor, and $J_{AF} \approx 0$. Thus, both the antiferromagnetic exchange integral in the layer and the ferromagnetic exchange integral between layers can be reasonably explained in terms of the topology of the bridges between copper atoms. Besides this, the values of these exchange integrals are comparable with the exchange integral values determined for other structurally related compounds. So, the antiferromagnetic intralayer exchange integral is similar to that obtained for copper formate tetrahydrate, $Cu(HCOO)_4{\cdot}4H_2O$,[42] (J/k = −35 K; T_{max} = 65 K) which, as has been previously discussed, presents a two-dimensional arrangement similar to that existing in the β-phase. On the other hand, the value of the ferromagnetic interlayer exchange integral is comparable to those obtained for the calcium copper formates (which behave as isolated one-dimensional ferromagnetic systems, with J_z/k = 0.30 and 0.47 K for $CaCu(HCOO)_4$ and $Ca_2Cu(HCOO)_6$, respectively) and to the interdimer exchange integral in the α-phase (J_d/k = 0.38 K), in which there exist similar bis(μ-oxo ligand) bridges between copper atoms.

The values of J_z for the two mixed formates follow the trend normally observed in related bis(μ-ligand) bridged compounds with regard to the relevant structural parameters, but the values of J_z (J_d) in β- and α-$[Cu(HCOO)_2]$ have been obtained from approximations and this prevents us from including these values in the correlation.

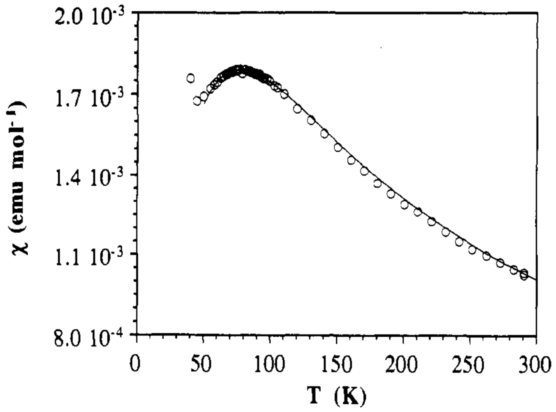

Figure 7. Magnetic susceptibility of β-$[Cu(HCOO)_2]$. The full line represents the fit to the series expansion (see text).

Finally, there are two mechanisms that can cause a canting of the magnetic moments.[43] The first one is due to an antisymmetric component of the superexchange interaction. The second source is the local anisotropy, which results in the existence of different preferential directions for the magnetic moments of ions in different sublattices. Both mechanisms can lead to canting in this compound, and a single-crystal magnetic characterization is needed in order to evaluate the contribution of each one to canting.

EPR Spectroscopy. The room-temperature powder EPR spectrum of α-$[Cu(HCOO)_2]$ consists of an exchange-narrowed single line (ΔH_{pp} = 40 Gauss) centered at a value of g = 2.16. When the temperature is lowered the only appreciable effect is that the signal intensity increases more quickly than that expected from the Curie law, according to the ferromagnetic nature of the compound. On the other hand, the room-temperature powder EPR spectrum of β-$[Cu(HCOO)_2]$ shows an unresolved broad (ΔH_{pp} = 350–400 G) band of axial type. The g values are only resolved at lower temperatures leading to $g_\parallel$ = 2.34 and $g_\perp$ = 2.08. These g values are those expected for axially distorted CuO_6 chromophores[26] and are very close to those observed in the related $Cu(HCOO)_2{\cdot}4H_2O$ compound ($g_\parallel$ = 2.35 and $g_\perp$ = 2.06).[44] Moreover, in fully agreement with the short range antiferromagnetic interactions (above T_c) found in the magnetic measurements, the intensity of the EPR signal clearly decreases below 80 K.

We have also characterized both formates by means of a novel technique, the magnetically modulated microwave absorption (MAMMA) technique, which is based on the detection of the in-phase change in microwave loss which is produced by the application of a small ac magnetic field to the sample.[25,45] The measurements can be made by using a conventional EPR spectrometer operating in the standard way. Due to the detection mode, only changes in microwave loss which are magnetic field dependent are observed. Until now, the only reported application of this technique was the observation of the superconducting transition,[25] but recently[45] we have shown that the MAMMA technique also can be very useful for the characterization of other magnetic field dependent phenomena such as transitions between a paramagnetic phase and a magnetically ordered one, which is the case we are dealing with.

Shown in Figure 8 is the MAMMA response of the studied compounds. In good agreement with the susceptibility results, the transition to the magnetically ordered phase is seen in the MAMMA spectrum as a sharp peak in the case of the β-$[Cu(HCOO)_2]$ compound. In the case of α-$[Cu(HCOO)_2]$ compound the transition peak is, however, less defined due to problem in stabilizing the temperature below 10 K in our variable temperature device.

---

(40) De Jongh, L. J. In *Magnetic Properties of Layered Transition Metal Compounds*: de Jongh, L. J., Ed.; Kluwer Academic Publishers: Dordrecht, The Netherlands, 1990; pp 1–51.

(41) Renard, P. J. In *Organic and Inorganic Low-Dimensional Crystalline Materials*; Delhaes, P., Drillon, M., Eds.; NATO ASI Series; Reidel: Dordrecht, The Netherlands, 1987.

(42) Seehra, M. S. *Phys. Lett.* **1969**, *28A*, 754.

(43) Moriya, T. In *Magnetism*: Rado, G. T., Suhl, H., Eds.; Academic Press: New York 1963; Vol. 1 p 85.

(44) Shimada, J.; Abe, H.; Ono, K. *J. Phys. Soc. Jpn.* **1956**, *11*, 137.

(45) Folgado, J. V.; Sapiña, F.; Beltrán, D. Manuscript in preparation.

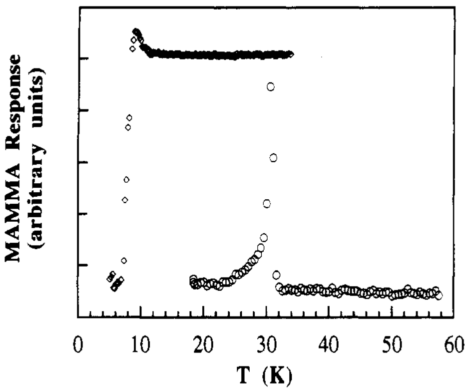

Figure 8. Microwave absorption of α (◇) and β (○) phases as a function of temperature.

Concluding Remarks. The obtaining of single crystals of β-[Cu(HCOO)$_2$] has allowed us to determine the crystal structure of this phase. It must be stated that the structural model proposed previously from powder data by Günter[17] is consistent with our results. Metastability of the β phase, which slowly transforms into the α phase at room temperature, has been confirmed, and on the basis of the structural relationships between the structures of these two polimorphs, a essentially distortional model for the phase transformation has been proposed. The magnetically modulated microwave absorption (MAMMA) technique has been used to detect the existence of 3d magnetic phase transitions in these two compounds, and these results are in good agreement with those obtained from magnetic measurements.

Finally, it must be stressed that these two anhydrous copper(II) formates behave as molecular ferromagnets with critical temperatures of 8.2 and 30.4 K, being two of the simplest ones characterized until now. α-[Cu(HCOO)$_2$] shows ferromagnetism, whereas β-[Cu(HCOO)$_2$] shows weak ferromagnetism. The application of the theory of Bertaut has showed the compatibility between the observed magnetic behavior and the crystal structure of these two polimorphs. Both of these magnetic behaviors and the observed T_c values are really remarkable in the field of magnetochemistry.

Acknowledgment. We are very indebted to Luis Lezama (Universidad del Pais Vasco, Bilbao, Spain) for the dc susceptibility and magnetization measurements. This research was supported by the Spanish Comisión Interministerial de Ciencia y Tecnología (CICYT, MAT 90-1020 and MAT 93-0240).

Supplementary Material Available: Tables S1–S3, giving crystal data and details of the structure determination, atom coordinates and anisotropic thermal parameters, and bond lengths and bond angles (3 pages). Ordering information is given on any current masthead page.